A R C H I V E S O F M E T A L L U R G Y A N D M A T E R I A L S
Volume 60 2015 Issue 4
DOI: 10.1515/amm-2015-0455

J. WIECZOREK*,#, B. OLEKSIAK**, J. MIZERA***, K. KULIKOWSKI****, P. MAJ***

EVALUATION OF THE QUALITY OF COATINGS DEPOSITED ON AZ31 MAGNESIUM ALLOY USING THE ANODISING METHOD

OCENA JAKOŚCI POWŁOK WYKONANYCH NA STOPIE MAGNEZU AZ31 METODĄ ANODOWANIA

The paper presents results of a study on the quality of coatings deposited on surfaces of AZ31 magnesium alloy products. In order to obtain protective coatings (corrosion and erosive wear protection), the methods of anodising (specimens A, B and C) and, for comparison, electroless plating (specimen D) were applied. The assessment of coating quality was based on the scratch test results. The results were used for determination of critical loads resulting in coating rupture. The best result was obtained for the specimen B (sulphuric acid anodising in combination with sealing): the critical load was 7.5 N. The smallest value (5.5 N) was observed for the specimen D, i.e. the coating produced using the electroless plating method. Moreover, erosion resistance of the coatings was assessed. In this case, a depth of the wear trace due to an erodent agent (SiC powder) effects was investigated. The results are comparable to those obtained in the scratch test. The poorest erosion resistance is demonstrated by the coating D and the best resistance is observed for the coating B.
Keywords: magnesium alloys, protective coatings, anodising, scratch test, erosion testing

W artykule przedstawiono wyniki badań jakości powłok wytworzonych na powierzchni wyrobów ze stopu magnezu AZ31. Dla wytworzenia powłok o charakterze ochronnym (ochrona przed korozją i zużyciem erozyjnym), zastosowano metodę anodowania (próbki A, B i C) oraz dla porównania metodę bezprądową (próbka D). Ocenę jakości powłok oparto o wynik próby zarysowania (scratch-test). Na podstawie uzyskanych wyników wyznaczono krytyczne obciążenie, przy którym następuje przebicie powłoki. Najlepszy wynik uzyskano w przypadku próbki B (anodowanie w kwasie siarkowym połączone z uszczelnianiem), wartość krytycznego obciążenia wynosiła 7.5 N. Najmniejszą wartość obciążenia krytycznego 5.5 N, zarejestrowano w przypadku próbki D tj. powłoki wytworzonej bezprądowo. Oceniono także odporność powłok na zużycie erozyjne. W tym przypadku badano głębokość śladu powstałego wskutek oddziaływania na powierzchnię próbek ścierniwa (proszek SiC). Uzyskane wyniki są podobne do zarejestrowanych w próbie zarysowania. Najmniejszą odpornością na erozję charakteryzuje się powłoka wytworzona bezprądowo (D) a największą powłoka anodowana i uszczelniana (B).

1. Introduction

Most of common magnesium alloys are based on a binary magnesium-aluminium system. Over the last decade, Mg-Al-Zn (AZ) alloys have been of special interest due to their good tensile strength, atmospheric corrosion resistance, good casting properties and small production costs compared with other magnesium alloys. This set of properties makes the AZ alloys useful materials for certain structural applications in the aerospace, automotive and electronic industries [1-4]. Other advantages of Mg-Al-Zn alloys, as well as of other light-metal alloys like Ti and Al, and of the composites based on their matrixes, are: a high damping coefficient, size stability, stiffness and a high recycling potential [2, 6-10]. It is estimated that in the nearest future, magnesium alloy applications will increase yearly by about 15–20%, mainly as complementary for advanced composite materials used in aviation industry [11-14]. At present, the AZ31 alloy is of a very high practical importance among magnesium casting alloys due to its good strength and plastic properties as well as high corrosion resistance and wear resistance [15-17]. It is used for production of rolled articles (i.e. strips, sheets) and extruded products [4, 9, 15]. Basic strength properties of the AZ31 alloy are presented in Table 1 [1, 4, 13, 18, 20].

* SILESIAN UNIVERSITY OF TECHNOLOGY, FACULTY OF MATERIAL SCIENCE AND METALLURGY, INSTITUTE OF MATERIALS SCIENCE, 8 KRASIŃSKIEGO STR., 40-019 KATOWICE POLAND

** SILESIAN UNIVERSITY OF TECHNOLOGY, FACULTY OF MATERIAL SCIENCE AND METALLURGY, INSTITUT OF METALS TECHNOLGY, 8 KRASIŃSKIEGO STR., 40-019 KATOWICE, POLAND

*** WARSAW UNIVERSITY OF TECHNOLOGY, FACULTY OF MATERIALS SCIENCE AND ENGINEERING, DIVISION OF MATERIALS DESIGN, 141 WOŁOSKA STR., 02-507 WARSZAWA POLAND

**** WARSAW UNIVERSITY OF TECHNOLOGY, FACULTY OF MATERIALS SCIENCE AND ENGINEERING, DIVISION OF SURFACE ENGINEERING, 141 WOŁOSKA STR, 02-507 WARSZAWA, POLAND

Corresponding author: jakub.wieczorek@polol.pl

TABLE 1
Physical and mechanical properties of the AZ31 alloy

AZ31 alloy properties		Value	Symbol	Unit
Physical properties	Density	1.78	ρ	g/cm^3
Mechanical properties	Tensile strength	250 – 290	R_m	MPa
	Conventional yield point	150 – 220	$Rp_{0.2}$	MPa
	Hardness	46 – 73	HB	
	Elongation	12 – 21	A5	%

Anodising of magnesium and its alloys is one of the most effective methods of corrosion prevention and, therefore, it is a commonly used process. Various types of coatings, produced under specific electric current conditions (the major process parameters), have been developed. A protective coating is a result of a chemical reaction between the anode substrate, oxygen, electrolyte and other components of the bath [18-19]. When a voltage is applied, the electrolyte near the anode surface is heated to a high temperature that allows for complex chemical (coating deposition), electrochemical (magnesium alloy oxidation) and physical (high-temperature component deposition) reactions [16, 18-19]. In the anodising process, the key factor that differentiates specific methods is the type of applied electrolyte. It highly influences the quality and intended use of the coating. So far, a lot of methods for anodising of magnesium and its alloys have been developed. Parameters of selected processes, described in literature sources, are presented in Table 2.

The examples of coating processes, presented in Table 2, are conventional solutions that have been modified for many years to yield better coating parameters and to reduce production costs or the environmental impact of the applied technologies [1]. Types of coating that is based on the conventional Dow 17 and HAE processes as well as meets current requirements regarding the aerospace and automotive industries are the Tagnite® and Eltron's coatings [1]. Electrolytes that are used in these processes contain less harmful substances such as chromic acid, permanganates, fluorides or other heavy metals [15, 18-20]. At present, a lot of research on compositions of alkaline baths with additions of phosphates, silicates, borates and organic substances is conducted [15-16]. However, to obtain an effective anodic coating, proper electrical parameters must be selected.

2. The coating process

The coatings were deposited on the AZ31 casting magnesium alloy. Its chemical composition is presented in Table 3.

TABLE 3
Chemical composition of the AZ31 alloy as per the ASTM standards [18, 20]

Chemical composition [%]				
Mg	Al	Zn	Mn	Cu
The other fraction	2.5 - 3.5	0.7 – 1.3	0.2 – 1.0	0.05

The investigations were performed using 4 specimens of starting material: onto 4 discs (30 mm in diameter), protective coatings were deposited. In Table 4, the process parameters are presented.

TABLE 2
Parameters of anodising processes [1, 18-20]

Type of the process	Bath composition [g/l]	Temperature [°C]	Current density [A/dm^2]	Time [min] / Voltage [V]	Comments
HAE	120 KOH 35 KF 20 $KMnO_4$ $34Al(OH)_3$ $35Na_3PO_4$	21-30	1.2-1.5	90/85	Opaque, brown, hard, brittle coating; corrosion and abrasion resistant; 25–50 µm
Dow 17	360 $(NH_4)HF_2$ 100 $Na_2Cr_2O_7$ 97 H_3PO_4	70-85	0.5-5	10–100/ max110	Opaque, dark green coating; corrosion and abrasion resistant; thickness: 25 µm
TAGNITE	4-8 KOH 5-10 KF 15-25 silicate	4-16	-	-	White coating; pH 12.8–13.2
Alkaline solution with sodium silicate additive	40 NaOH 90 Na_2SiO_3	20	1	30/-	Corrosion resistance improvement

TABLE 4
Process parameters of coating deposition onto the AZ31 alloy specimens

Specimen no	Electrolyte type	Current density [A/cm^2]	Time [min]	Comments
A	5g/l H_2SO_4	0.13	3	H2SO4 anodising
B	5g/l H_2SO_4	0.13	3	Anodising, sealing 100°C/30min/ water
C	5g/l H_2SO_4 3g/l $KMnO_4$	0.275	3	Anodising, sealing 100°C/30min/ water
D	10 g/l $C_6H_8O_7$	0	720	Electroless coating

Before placing in the electrolyser, the specimens were polished and degreased. The electrolyte was a 5 g/l aqueous solution of sulphuric acid. Due to high reactivity of the magnesium specimen, a low solution concentration was selected. When higher concentrations were applied, the magnesium alloy was too rapidly dissolved by the acid. The specimen was connected to the positive pole as the anode. The cathodes, i.e. stainless steel plates, were connected to the negative pole. The target current density was 0.13 A/cm^2. The anodising process was carried out for 3 minutes at the ambient temperature. After three minutes, the system was disconnected; then, the specimen was rinsed with distilled water and air-dried (Fig. 1a). Following the anodising process, the specimen B was immersed in 100°C water for 30 minutes in order to seal the coating. Regarding the specimen C (Fig. 1c), $KMnO_4$ was added to the electrolyte. Potassium permanganate was used due to its strong oxidising effects. The procedure was partially inspired by environmetal friendly treatment of natural reinforcing fibres for composites [19-21]. Following the anodising process, the specimen was sealed. The resulting layer was darker and less uniform than those obtained for the specimens anodised without $KMnO_4$. The specimen D was subjected to electroless plating through immersing in a 10 g/l citric acid solution for 24 hours to produce an opaque, light coating on the specimen surface (Fig. 1d).

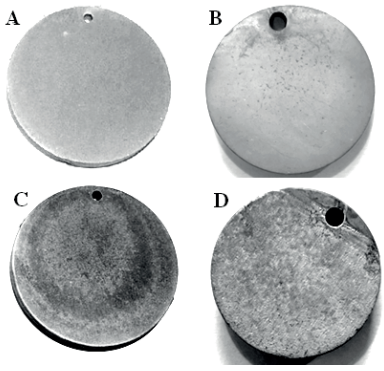

Fig. 1. The specimens following the coating process

3. Scratch test

The evaluation of produced layer quality was based on results of scratch resistance testing by means of the scratch test. The test was performed using a CSM tester with a diamond indenter (spherical tip radius 200 μm; Rockwell, no. C-233). During the test, the specimen surface was scratched with an indenter of known stylus geometry. The specimen is moved at a constant velocity perpendicular to the stylus which, when a defined force is applied, penetrates its surface. Throughout the test, contact force, penetration depth, friction force, acoustic signal related to cracking and detaching of the coating were measured. The analysis of the layer adhesion strength was based on a microscopic observation and profilometric measurements of the scratch. As a result, the critical load that leads to characteristic defects was determined. Moreover, an analysis of the friction coefficient changes was performed and the critical load (LcW), corresponding to the layer rupture, was determined. Also, the critical load (LcO), based on the analysis of the wear trace, was specified. The critical load values, at 1 N to 15 N, were identified based on three test runs. Durability and a quality of the obtained coating can be compared when the wear trace length until the substrate exposure is determined. Mean critical load values are presented in a bar chart (Fig. 2). Mean values of the friction coefficient, measured during the scratch test, are presented in Figure 3.

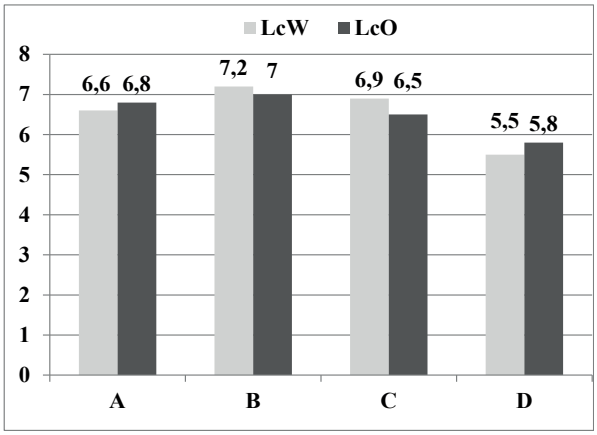

Fig. 2. Critical loads for the investigated coatings at 1 N to 15 N: (LcW – critical load resulting from the friction force analysis, LcO – critical load determined in the wear trace analysis)

In Figure 4a, a 3D image of the wear trace at the coating A (anodised in sulphuric acid) rupture location is presented. While analysing the microscopic image of the wear trace (Fig. 4c) and the profile height change (Fig. 4b), location of the coating rupture, following the distance of 3.5 mm, was determined. It corresponds to the critical load of 6.6 N.

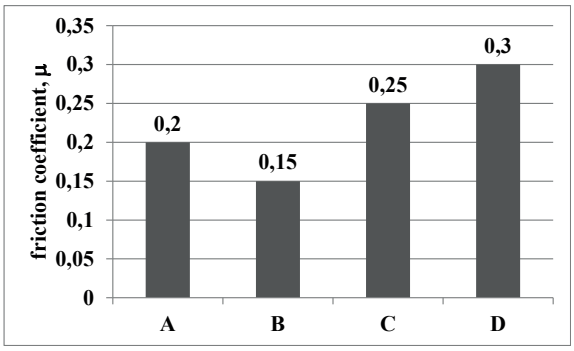

Fig. 3. Mean values of the friction coefficient for the range of 1 N to 15 N

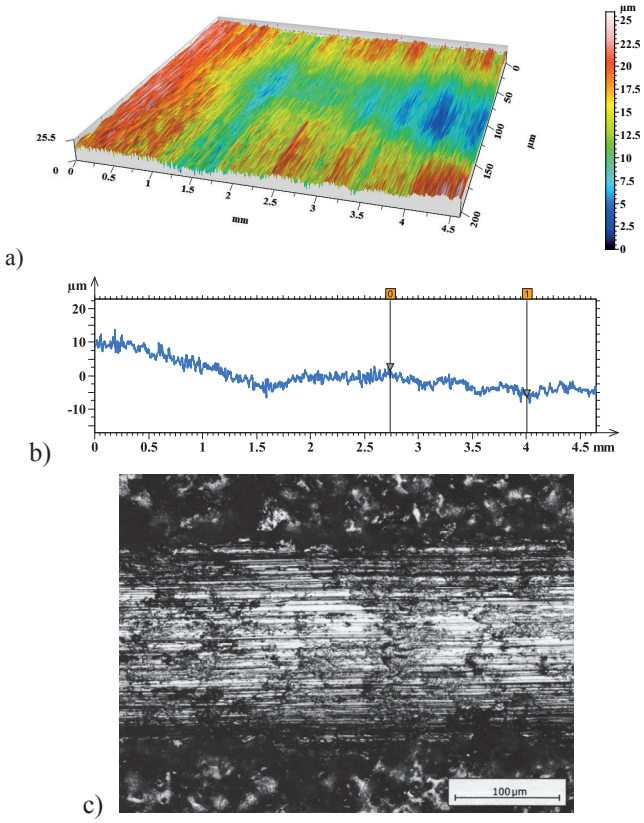

Fig. 4. Substrate exposure in the specimen A (distance: 3.5 mm): a) a 3D image of the surface topography, b) a 2D profile determined along the scratch, c) a microscopic image

In the case of coating B (a result of anodising and sealing processes), the coating rupture location was observed following the distance of 6 mm (Figs. 5a, 5b), which corresponds to the critical load of 7.2 N.

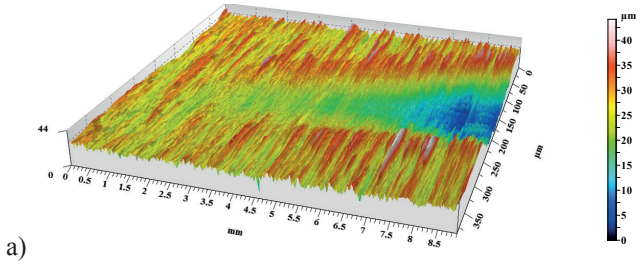

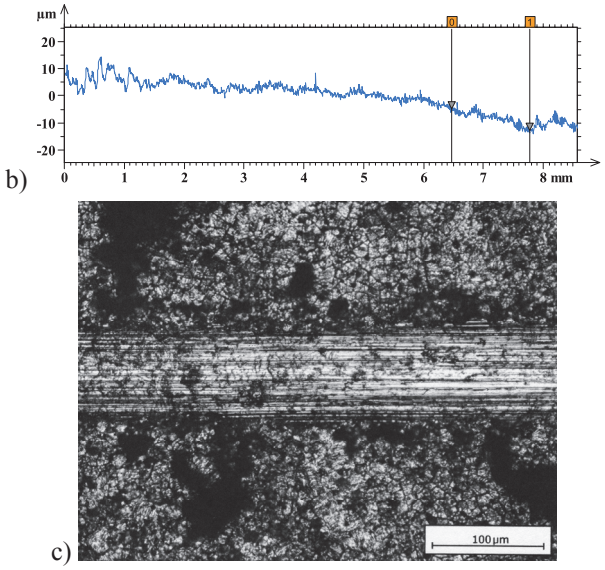

Fig. 5. Substrate exposure in the specimen B (distance: 6.5 mm): a) a 3D image of the surface topography, b) a microscopic image

For the specimen C (anodising with addition of KMnO4 and sealing), the coating rupture was observed following the distance of 4.5 mm (Figs. 6a, 6b), corresponding to the critical load of 6.9 N (comparable to the result for the coating B). The wear trace on the specimen C surface shows no cracks or disconuities that are observed for the specimen B (Figs. 5c and 6a).

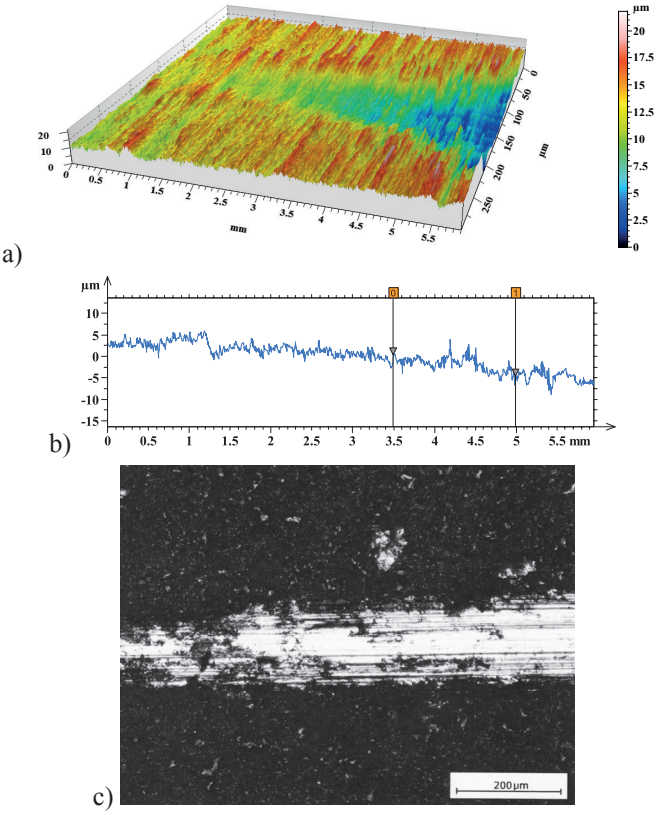

Fig. 6. Substrate exposure in the specimen C (distance: 4.5 mm): a) a 3D image of the surface topography, b) a 2D profile determined along the scratch, c) a microscopic image

The last investigated coating (specimen D) was obtained using the electroless plating method. Its scratch resistance

was the poorest of all investigated specimens. In Figure 7, the coating D rupture location, following the distance of 3 mm, is presented. In this case, the critical load is 5.5 N. The electroless coating demonstrates a high roughness level and discontinuity of the wear trace.

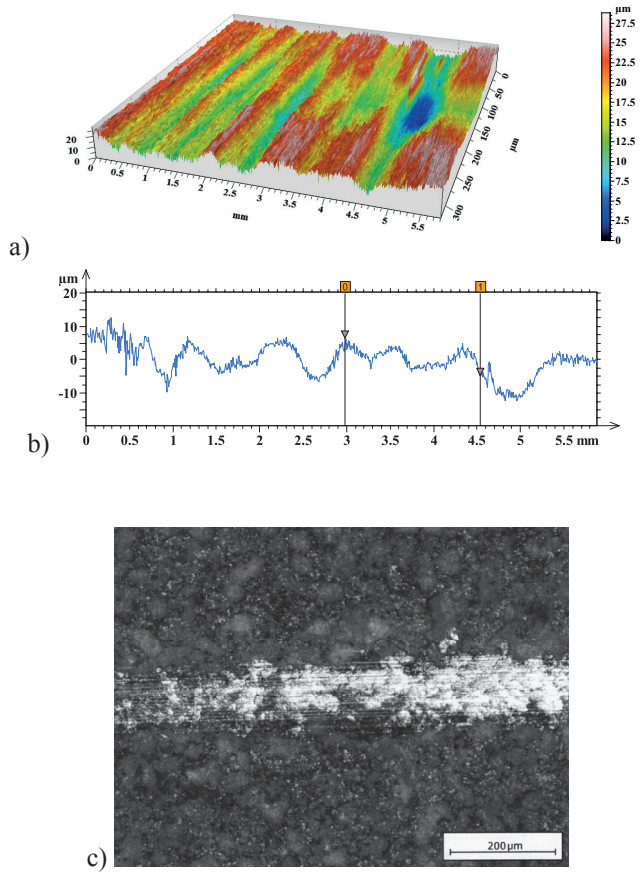

Fig. 7. Substrate exposure in the specimen D (distance: 3 mm): a) a 3D image of the surface topography, b) a 2D profile determined along the scratch, c) a microscopic image

For the tested coatings, surface roughness levels were determined based on profilographometric measurements. The results were expressed as the Ra parameter values in a bar chart (Fig. 8). The lowest level of surface roughness was observed for the coating A (Ra=1), while the highest level (over 2-fold higher) was found for the coating D (Ra=2.2).

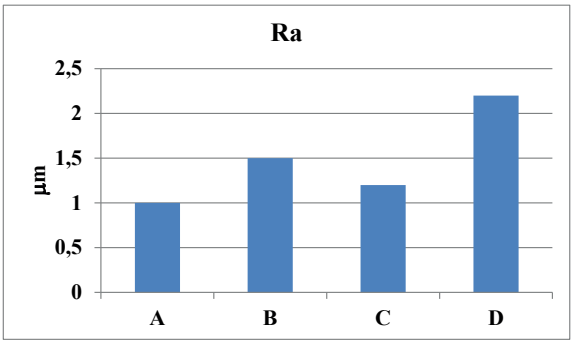

Fig. 8. A comparison of surface roughness levels for the AZ31 alloy specimens following the coating process

4. Erosion resistance testing

In order to determine performance characteristics of the produced coatings, erosive wear tests were performed. Due to potential applications of the magnesium alloy products in the aerospace industry, it was assumed that in addition to corrosion, erosive wear would be the essential factor affecting the coating durability. For each investigated specimen, two tests were carried out. During each test, 2 grams of an erodent agent were applied to the specimen at 45° for 1 minute. An image of the test device is presented in Figure 9 [7, 10, 15].

Fig. 9. A device for erosive testing of the coatings

Wear traces, observed on the specimen surfaces, are shown in Figure 10. For the purpose of wear trace quantitative assessment, profilographometric measurements were performed to determine its size and depth. The size measurement results, based on the surface topography analysis, are presented in Table 5. The deepest trace of 35 µm was observed for the electroless coating D, which suggests its poor erosion resistance (Fig. 11b). The smallest value of 27 µm was found for the coating B (anodising combined with sealing) (Fig. 11a). The results are consistent with the scratch test outcomes.

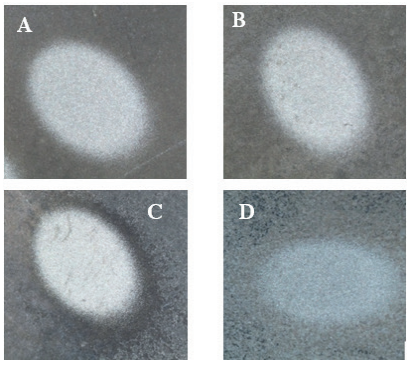

Fig. 10. Wear traces observed on the specimen surfaces following the erosive wear test

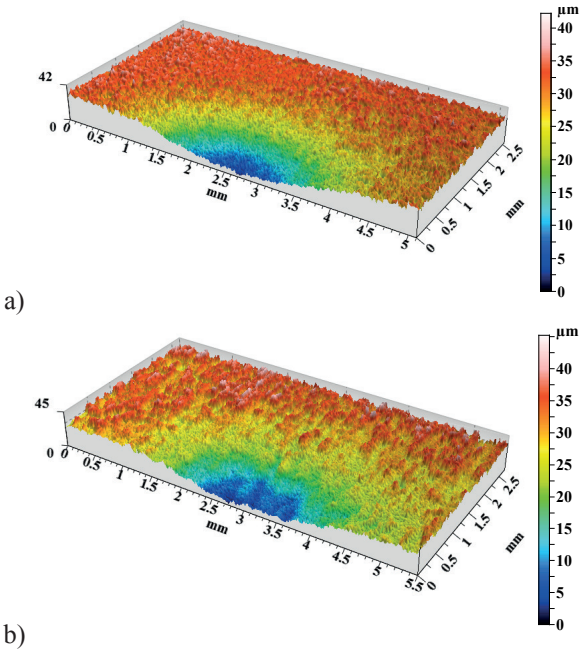

Fig. 11. Topographies of the wear traces on the specimen surfaces: a) specimen A, b) specimen D

TABLE 5

Sizes of erosive wear traces

Specimen label	Wear trace depth, µm	Surface area of the wear trace, mm^2
A	3.2	18
B	2.7	16
C	2.9	17
D	3.5	20

5. Summary

The investigations allowed for assessment of the quality of protective coatings produced by means of various techniques. Based on the profilometric measurements, differences in the roughness levels of the coatings were determined. The differences are considerable and affect the coating durability. The highest level of roughness is observed for the coating D (obtained by means of the electroless plating method) which also shows the poorest scratch resistance. This result suggests no practical applications for this type of coating. However, a highly rough coating, obtained with the use of electroless plating technology, may be successfully used as an interlayer in the polymer-based coating processes regarding structural elements. This promotes enhancement of the polymer layer - substrate bonding. The electroless plating method is cheap and environmentally friendly. For elements of more complex geometry, it is easier to be performed, for the purpose of surface preparation, than mechanical working. In the group of anodic coatings, the highest level of durability is observed for the specimen B resulted from anodising combined with sealing in 100°C water. It shows the highest durability determined in the scratch test (a 6 mm distance until the coating rupture). Moreover, this type of coating demonstrated the most favourable result of erosive wear testing. Compared with the anodic coating A, the coating B shows a higher level of surface roughness and it is less aesthetic. The coating A demonstrates the lowest scratch and erosion resistance in the group of anodic coatings. Its advantage is a light, uniform colour and a low roughness level (Ra=1.0). The aesthetic values of this coating can be considered for applications with poor tribological effects, for example to protect vehicle interior elements (dashboards, seats etc.). Summing up the research results, it can be concluded that despite the differences in wear resistance and surface quality of the obtained coatings, their practical applications are possible.

Acknowledgements

The study was conducted under the Research Project No. POIG.01.01.02-00-015/08-00,

FSB-34/RM2/2009ZB711/020/FSB09/0001-07, financed by the Ministry of Science and Higher Education – Poland.

REFERENCES

[1] L. Chai, X. Yu, Z. Yang, Y. Wang, M. Okido, Anodising of magnesium alloy AZ31 in alkaline solutions with silicate under continuous sparking, Corrosion Science **50**, 3274-3279 (2008).

[2] T. Rzychoń, M. Dyzia, I. Pikos, Microstructure of WE43 magnesium matrix composite reinforced with ceramic particles **211**, 101-108 (2014).

[3] T. Rzychoń, B. Adamczyk-Cieślak, A. Kiełbus, J. Mizera, The influence of hot-chamber die casting parameters on the microstructure and mechanical properties of magnesium-aluminum alloys containing alkaline elements, Materialwissensch. Werkstofftech **43** (5), 421-426 (2012).

[4] D. Kuc, E. Hadasik, I. Schindler, P. Kawulok, R. Śliwa, Characteristics of plasticity and microstructure of hot forming magnesium alloys Mg-Al-Zn type, Archives of Metallurgy and Materials **58** (1), 151-156 (2013).

[5] A. J. Dolata, Hybrid Composites Shaped by Casting Methods, Light Metal and their Alloys III, Solid State Phenomena **211**, 47-52 (2014).

[6] A. J. Dolata, M. Dyzia, Effect of chemical composition of the matrix on AlSi/SiCp+Cp composite structure, Archives of Foundry Engineering **14** (1), 135-138 (2014).

[7] W. Simka, A. Sadkowski, M. Warczak, A. Iwaniak, G. Dercz, J. K. Michalska, A. Maciej, Characterization of passive films formed on titanium during anodic oxidation, Electrochimica Acta **56** (24), 8962-8968 (2011).

[8] A. Szkliniarz, W. Szkliniarz, Microstructure and properties of Ti-47Al-2W-0.5Si cast alloy, Solid State Phenomena **226**, 3-6 (2015).

[9] W. Szkliniarz, Nowoczesne materiały metaliczne - teraźniejszość i przyszłość, Wydział Inżynierii Materiałowej i Metalurgii Politechniki Śląskiej, Katowice (2009).

[10] A. Iwaniak, M. Sozańska, Badania odporności korozyjnej i erozyjnej powłok natryskiwanych cieplnie na stopie magnezu AZ91, Ochrona przed Korozją **5**, 204-209 (2014).

[11] M. Koziol, Experimental study on the effect of stitch arrangement on mechanical performance of GFRP laminates manufactured on a basis of stitched preforms, Journal of Composite Materials **46** (9), 1067-1078 (2012).

[12] A.J. Dolata, M. Dyzia, W. Walke, Influence of Particles Type and Shape on the Corrosion Resistance of Aluminium Hybrid Composites, Light Metals and their Alloys II, Solid State Phenomena **191**, 81-87 (2012).

[13] T. Rzychoń, B. Dybowski, A. Kiełbus, The influence of strontium on the microstructure of cast magnesium alloys containing aluminum and calcium, Archives of Metallurgy and Materials **60** (1), 167-170 (2015).

[14] M. Niklewicz, A. Smalcerz, A. Kurek, Estimation of system geometry and inductor frequency importance in induction hardening process of gears, Przegląd Elektrotechniczny **84** (11), 219-224 (2008).

[15] J. Przondziono, E. Hadasik, W. Walke, J. Szala, J.K. Michalska, J. Wieczorek, Resistance to electrochemical corrosion of the extruded magnesium alloy AZ80 in NaCl solutions, Materials Technology **49** (2), 275-280 (2015).

[16] J. Przondziono, W. Walke, E. Hadasik, J. Szala, J. Wieczorek, Corrosion resistance tests of magnesium alloy WE43 after extrusion, Metalurgija **52** (2), 243-246 (2013).

[17] K. Piwowar, A. Blacha-Grzechnik, R. Turczyn, J. Żak, Electropolymerized phenothiazines for the photochemical generation of singlet oxygen, Electrochimica Acta **141**, 182-188 (2014).

[18] Z. Shi, G. Song, A. Atrens, The influence of anodizing parameters on the corrosion performance of anodised coatings on magnesium alloy AZ91D, 13th Asian- pacific corrosion control conference (APCCC), Osaka, 1841-1846 (2003).

[19] G. Siwiec, B. Oleksiak, A. Smalcerz, J. Wieczorek, Surface tension of Cu-Ag alloys, Archives of Metallurgy and Materials **58** (1), 193-195 (2003).

[20] H. Dong, Surface engineering of light alloys, Woodhead Publishing Limited (2010).

[21] A. Bogdan-Wlodek, M. Koziol, J. Myalski, Influence of surface treatment on the wetting process of jute fibres with thermosetting polyester resin, Polish Journal of Chemical Technology **14** (1), 21-27(2012).

Received: 20 October 2014.